

Radiation Hardness Tests of GaAs preamplifiers

Joint Institute for Nuclear Research, Dubna, Russia:

A. Cheplakov, V. Golikov, S. Golubyh, V. Kukhtin, E. Kulagin, V. Luschnikov, A. Shalyugin

Max-Planck-Institut fuer Physik, Muenchen, Germany:

H.Brettel, W.D.Cwienk, J.Fent, L.Kurchaninov, H.Oberlack, P.Schacht

Abstract. A series of radiation hardness tests of GaAs preamplifiers has been performed at the IBR-2 reactor in Dubna. The preamplifier chips have been exposed to high fluence of fast neutrons and γ -dose. A stable performance of the electronics has been demonstrated up to a fluence of $5 \cdot 10^{14} \text{ n/cm}^2$ and a γ -dose of 55 kGy. The tests confirm the applicability of the preamplifiers for the ATLAS hadronic end-cap calorimeter.

1. Introduction

In the hadronic end-cap calorimeters of the ATLAS experiment [1] the radiation level of $0.3 \cdot 10^{14} \text{ n/cm}^2$ is expected after 10 years of LHC operation at high luminosity. Detailed studies of the GaAs preamplifier prototypes exposed to photons and fast neutrons at Dubna reactors have been carried out in 1996 [2]. No significant deterioration of the performance was observed for the neutron fluence up to $\sim 3 \cdot 10^{14} \text{ n/cm}^2$ and up to 31 kGy, the highest γ dose collected. The experiments were followed by the irradiation with neutron flux value less by two order of magnitude and no evidence for any dose rate effect was elucidated [3].

A series of radiation tests has been undertaken in 1999 with GaAs preamplifiers of the final design. There were three types of tests:

- 1) neutron irradiation of 7 chips. During the whole period of irradiation and measurements the motherboards with the GaAs chips were kept in the cryostat filled with liquid nitrogen. The preamplifiers were exposed to the total fluence of fast neutrons of $(1.11 \pm 0.15) \cdot 10^{15} \text{ n/cm}^2$ and a remaining γ dose of $(3.5 \pm 0.3) \text{ kGy}$. The measurements were

performed after the following dose steps (in 10^{14} n/cm^2 : 0, 0.5, 1.2, 1.9, 2.6, 3.2, 3.8, 4.4, 5.0, 5.6, 6.8, 9.2, 9.8 and 11.1). The neutron fluence values presented in this paper have been recalculated to 1 *MeV* equivalent fluence (see paper [2]).

- 2) γ irradiation of 8 chips was also carried out at cold conditions. The total γ dose of $(55 \pm 8) \text{ kGy}$ was accompanied by a fast neutron fluence of $(1.1 \pm 0.2) \cdot 10^{14} \text{ n/cm}^2$. The measurements were undertaken before the irradiation run and after dose steps of 21.1, 40.5 and 55.0 *kGy*.
- 3) neutron irradiation of 23 chips was carried out in the parasitic neutron beam. The maximal value of the total neutron fluence of $(7.7 \pm 0.8) \cdot 10^{14} \text{ n/cm}^2$ was collected in four steps. The underlying γ dose was $(7.0 \pm 0.7) \text{ kGy}$. It was not possible to install the cryostat at the parasitic beam area. Therefore the motherboards with the GaAs chips were irradiated at room temperature. After each irradiation step the motherboards were taken out from the irradiation area and put into the liquid nitrogen cryostat for the measurements.

The results of these tests are presented after a brief description of the irradiation facility and the measurement setup.

2. Description of the experiment

The schematic layout of the experiment is presented in Fig.1. In the first two tests the motherboards with GaAs chips were immersed into the liquid nitrogen cryostat which was located in front of the movable platform not far from the beam shutter. During the period of electronics measurements the beam was blocked and the signals were transferred via coaxial cables of $\sim 50 \text{ m}$ length. The motherboards with 23 chips were located for the measurements in the cryostat near the counting room and the cable length was in this case only 5 *m*.

The composition of the beam was determined by the beam filter. It was a 5 cm thick Pb absorber for the neutron beam which has been replaced for exposure by the γ 's by a n/γ converter consisting of a paraffin moderator interleaved with cadmium foils.

The setup for the electronics measurements was identical to the one used in the previous experiments. It is presented in Fig. 2. Step pulses from the generator were sent to the GaAs preamplifiers and signals from various output channels were fed into the shaper system and then to the digital scope which was read out by a personal computer.

Four GaAs chips were mounted on one preamplifier board. Each chip contains eight preamplifiers and two drivers. Outputs of four preamplifiers are fed into the driver input. In order to simulate the liquid argon gap of the hadronic endcap calorimeter, the capacitors (C_d) were mounted on the motherboard in parallel to the preamplifier input channels. Every chip used the same capacitance value for all its preamplifiers. It was either 10, or 100, or 220, or 330 *pF*.

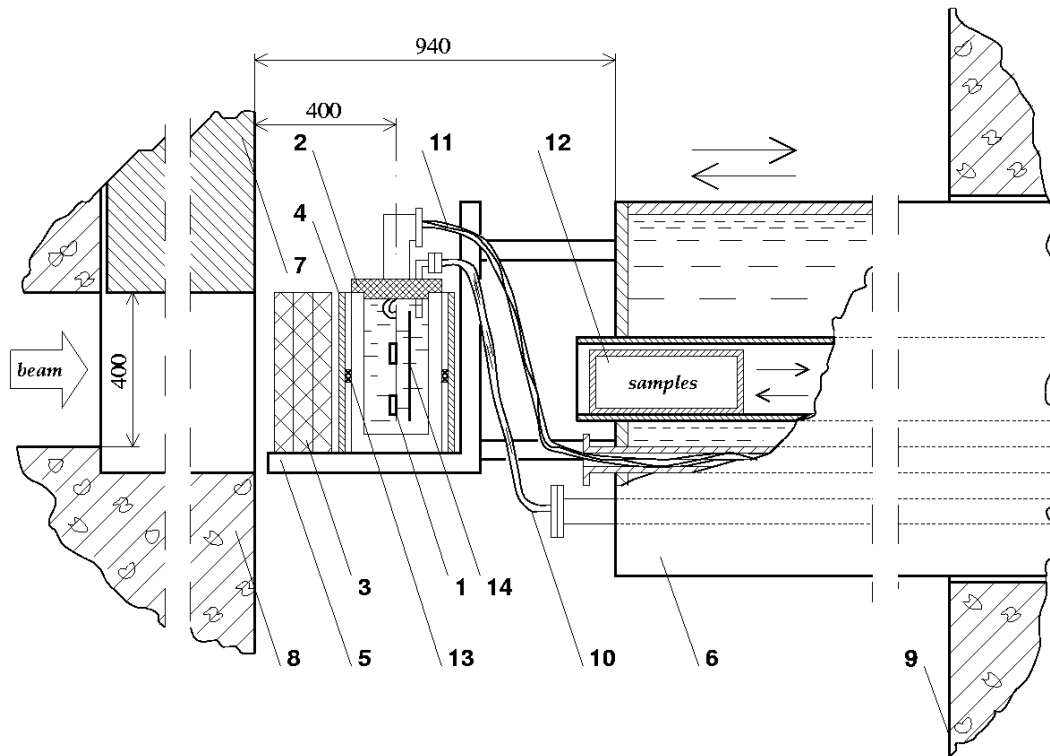


Figure 1: Schematic layout of the experimental setup: (1) cryostat, (2) measurement cables, (3) tube for samples transporting, (4) outer reactor shield, (5) boron carbide layer, (6) beam shutter, (7) beam filter, (8) neutron and γ dosimeters, (9) motherboard with the electronics (previous experiment), (10) nickel foil, (11) inner reactor shield, (12) support frame, (13) cryogenic lines, (14) movable shielding platform and (15) low dose rate position. The fast neutron flux at the beam axis (9) was $(1-9) \cdot 10^9$ n/cm²/s (dependent on the beam filter). It was about $1.5 \cdot 10^9$ n/cm²/s at the parasitic beam area (3) and $8 \cdot 10^7$ n/cm²/s at the low dose rate position (15) at the inner surface of the reactor shield.

The standard set of characteristics like transfer function, rise time, linearity and equivalent noise current (ENI) of preamplifiers were measured.

The transfer function was measured as the output voltage for different values of the input current. The rise time was defined as the time between signal level of 5% and the peak position. The r.m.s. voltage on the shaper output with no input signal was used to determine the noise value. All measurements were done for different values of the shaper time constant. The shaper allowed to vary the time constant in the range from 10 ns to 10 μ s. The linearity of the preamplifiers was measured for different channels by injecting triangular pulses with amplitudes in the range from 0 to 5 mA. All parameters were measured before the irradiation and after each step of the total dose.

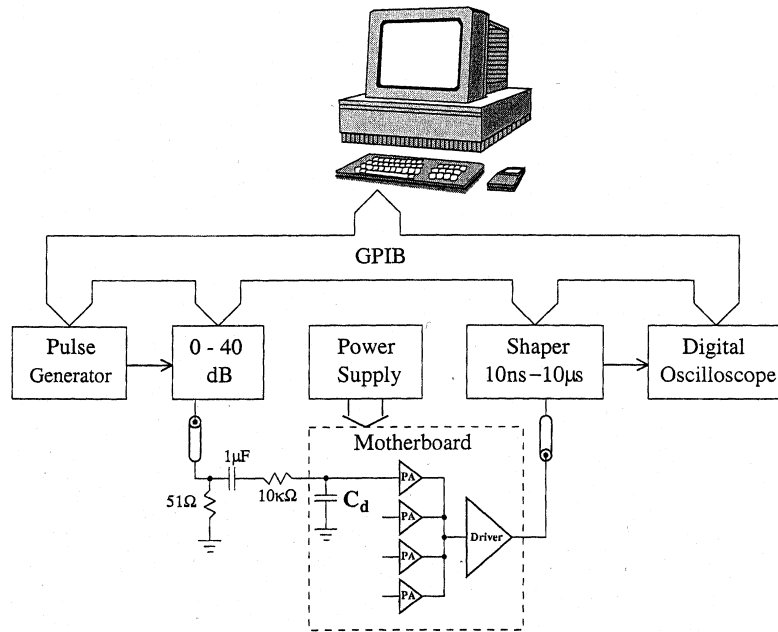


Figure 2: Schematic layout of the measurement setup.

One has to note that the experimental setup was sensitive to the pickup noise. The effect was most visible for channels with high C_d values and the affected data (~15% of all the measurements) were not used in the analysis. In order to suppress possible fluctuations and make the conclusion more evident, the measured parameters were averaged over the group of channels with the same detector capacitance. The averaged values will be shown in the following analysis of the transfer function, the rise time and the noise behaviour.

3. Experimental results

3.1 Transfer function and rise time

The transfer function measurement monitors the gain stability of the preamplifiers during the irradiation. The results of the measurements are presented for four groups of channels with different detector capacitance in Fig.3 for the neutron irradiation and in Fig.4 for the γ run. The data for various shaper time constants (10, 20, 50 and 100 ns) are normalised to those obtained before the irradiation.

A degradation of the transfer function by 20% of its initial value is observed at the neutron fluence level of $(5-6) \cdot 10^{14} \text{ n/cm}^2$ for different shaper time constants and detector capacitance values. In the previous tests [2] with the prototype chips such decrease of the transfer function was seen at $1 \cdot 10^{14} \text{ n/cm}^2$ for $C_d = 330 \text{ pF}$.

The transfer function is more stable for the γ irradiation. A small degradation at the highest γ dose is at the same level as one would expect for the integrated underlying neutron fluence of $1.1 \cdot 10^{14} \text{ n/cm}^2$.

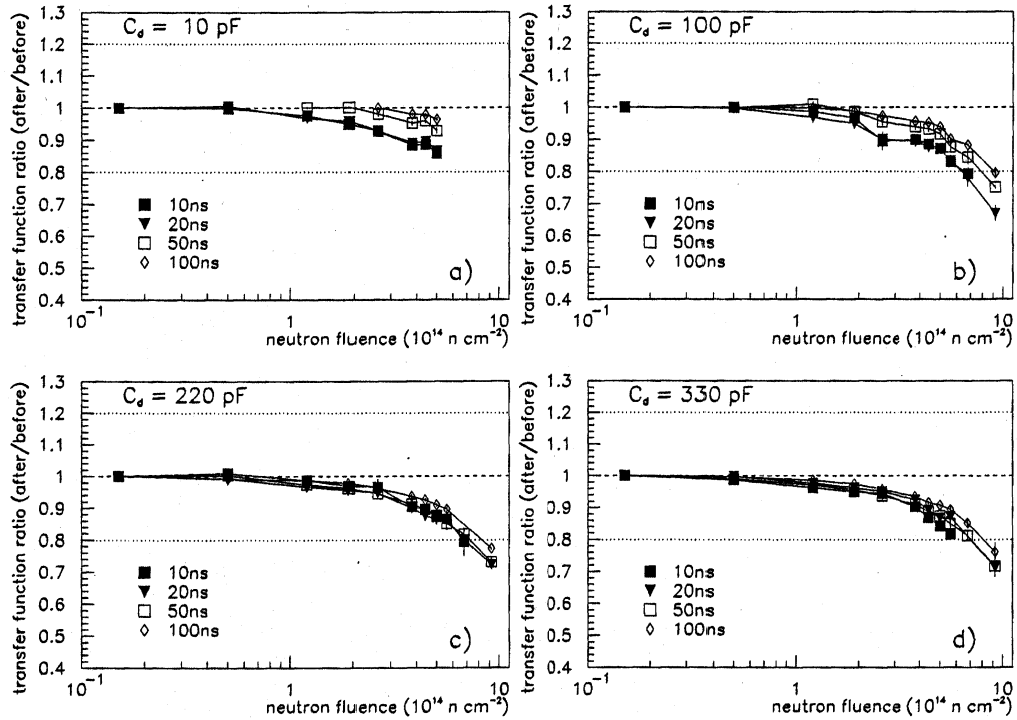


Figure 3: Ratio of the transfer function measured after various neutron fluences and before the irradiation. The ratio dependence is shown for four groups of preamplifiers with different detector capacitance and various values of the shaper time constant.

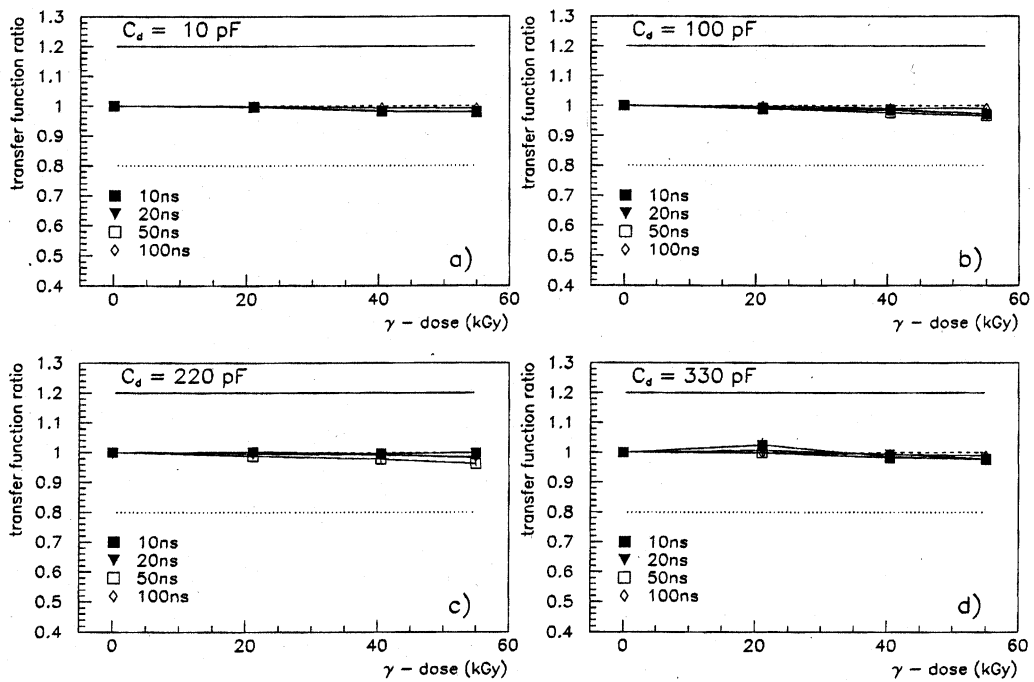


Figure 4: Ratio of the transfer function measured after various gamma-dose values and the transfer function before the irradiation. The ratio dependence is shown for four groups of preamplifiers with different detector capacitance and various values of the shaper time constant.

The r.m.s of the transfer function distributions for different detector capacitance and various shaper time constants measured during the neutron irradiation of 23 chips is shown in Fig.5. It is seen that the spread of the transfer function value is stable within $\pm 20\%$ up to the neutron fluence of $5 \cdot 10^{14} \text{ n/cm}^2$.

A similar conclusion can be drawn for the rise time behaviour with neutron fluence (Fig.6) and γ dose (Fig. 7), as well as for the r.m.s of the rise time values (Fig.8).

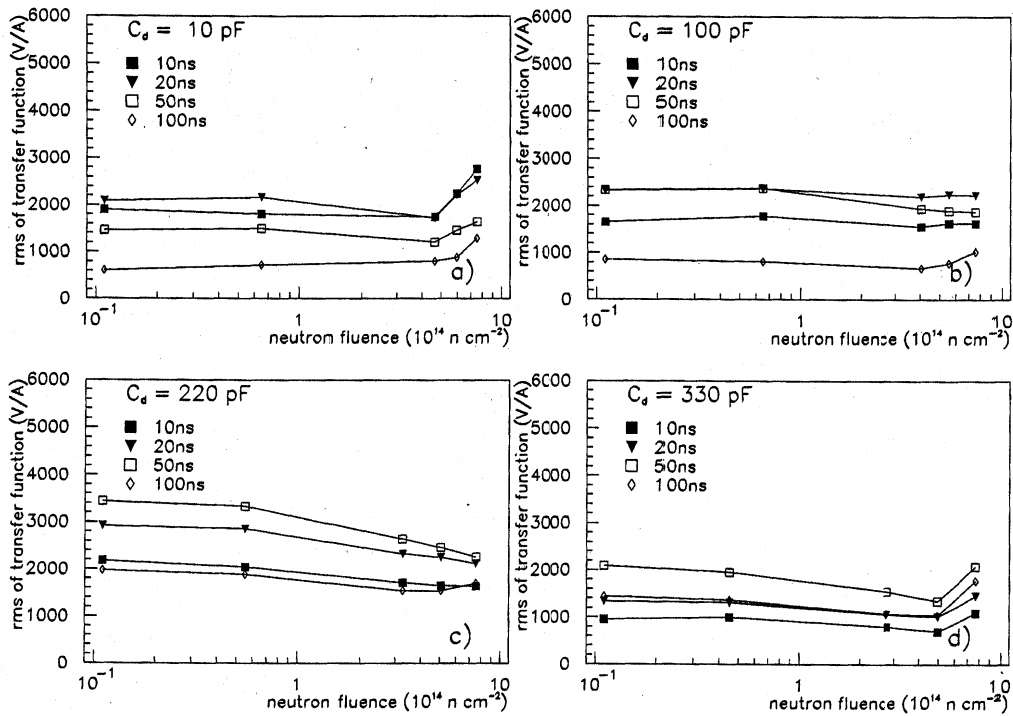


Figure 5: Spread of the transfer function values during the neutron irradiation of 23 chips.

3.2 Linearity

To measure the linearity, the step pulses from the range of 0-0.5 mA were injected in the preamplifier's input. The output signals were sent to the digital oscilloscope and read out by a personal computer. The results for the neutron and γ runs are shown in Fig.9 and Fig.10. The linear relation between the output voltage and the input current is seen in the interval from 0 to 0.4 mA (see left side of the Figures with data for the particular preamplifier with input capacitance of 220 pF). The linear fit was carried out after the various irradiation steps and for different preamplifiers in the input current interval of 0.4-250 μA (the LHC limit) which is marked by the arrow. The slope determines the gain of the preamplifier and is presented at the right side of the Figures for various detector capacitance values.

As it was observed in the previous tests with the prototypes, no degradation is seen for the γ irradiation. The preamplifiers withstand rather high neutron fluence of $5 \cdot 10^{14} \text{ n/cm}^2$ with a relatively small ($\sim 10\%$) loss of the gain.

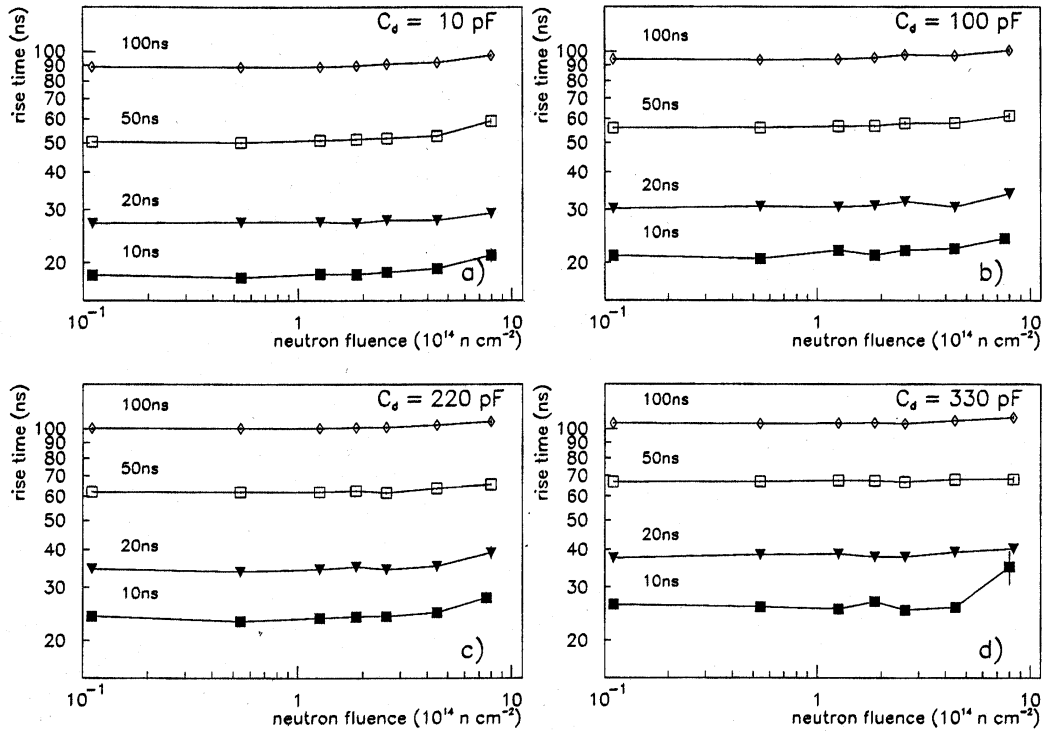


Figure 6: The rise time of the pulse after the shaper measured in the experiment as a function of the neutron irradiation level. The data are presented for four groups of preamplifiers with different detector capacitance and various values of the shaper time.

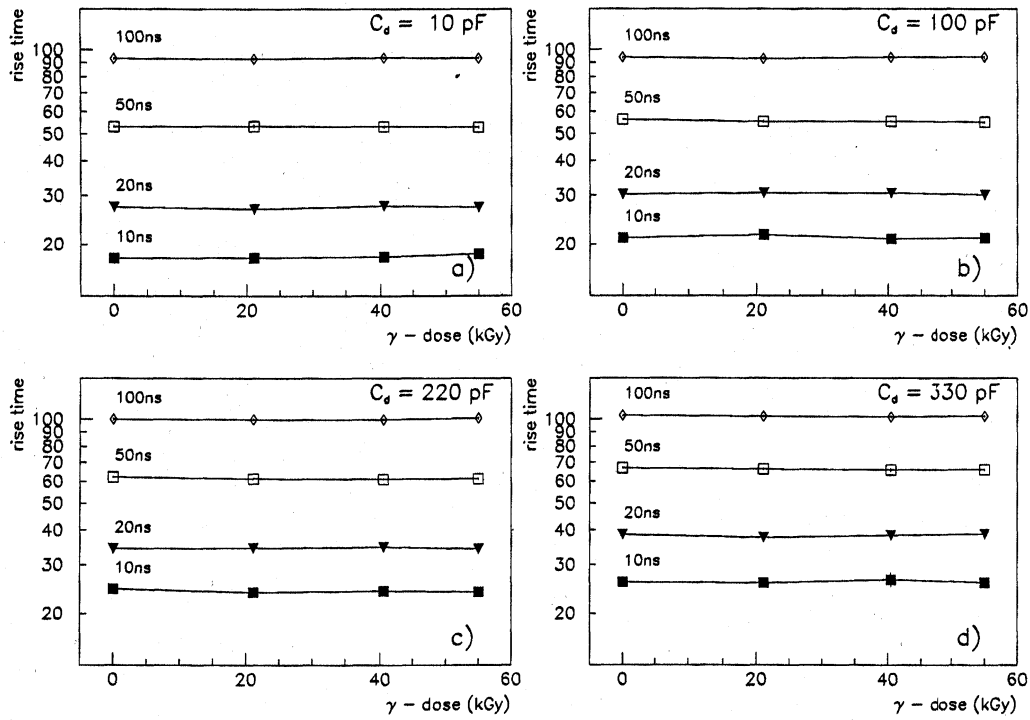


Figure 7: The rise time of the pulse after the shaper measured as a function of the γ dose. The data are presented for four groups of preamplifiers with different detector capacitance and various values of the shaper time.

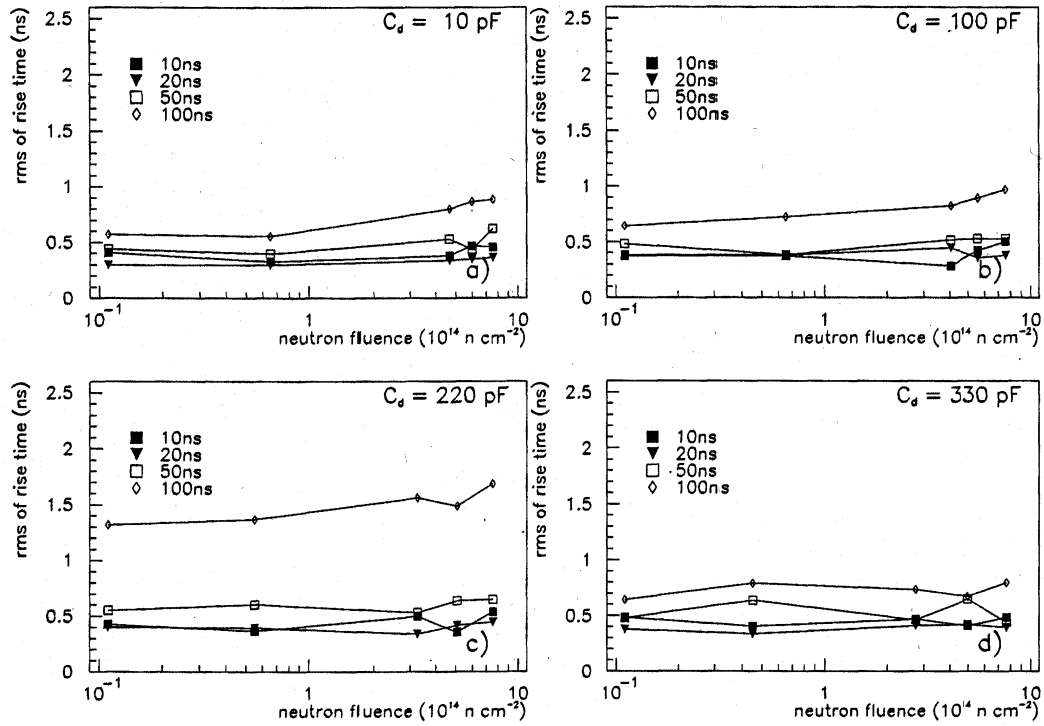


Figure 8: Spread of the rise time values measured after the shaper during the neutron irradiation of 23 chips.

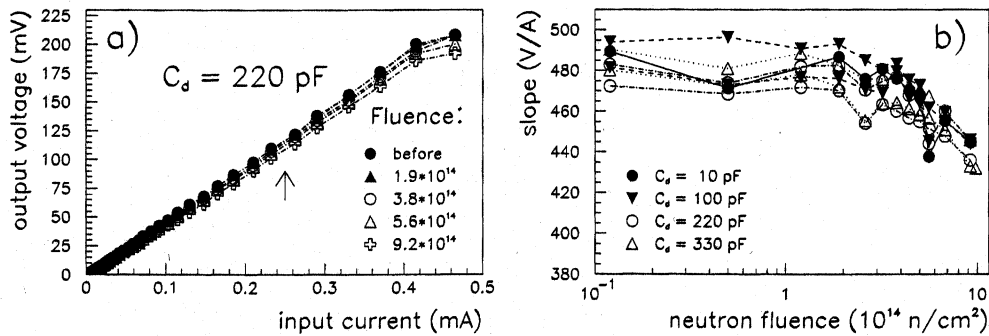


Figure 9: (a) The measured linearity for a preamplifier with $C_d = 220$ pF and the corresponding slope of the linear fit up to $250 \mu\text{A}$ as a function of the neutron fluence. (b) The slope obtained for different detector capacitances.

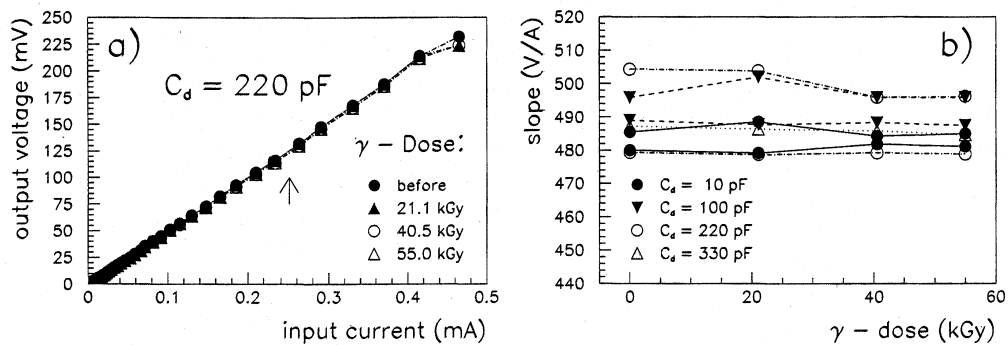


Figure 10: (a) The measured linearity for a preamplifier in the γ run and the corresponding slope of a linear fit up to $250 \mu\text{A}$ as a function of the γ dose. (b) The slope obtained for different detector capacitances.

The linearity was measured also in the neutron irradiation of 23 chips. The results of the linear fit for the preamplifiers with different detector capacitance values are shown in Fig.11a. The data were corrected by taking into account a weak dependence of the preamplifier's gain on the input capacitance value. These corrections are: +1.8, +8.6 and +16.1 V/A for 100, 220 and 330 pF respectively.

The r.m.s of the slope values is presented in Fig.11b as a function of the neutron fluence. It is seen that the spread of the preamplifier gain values is stable within $\pm 20\%$ up to the neutron fluence of $5 \cdot 10^{14} \text{ n/cm}^2$ for various detector capacitances.

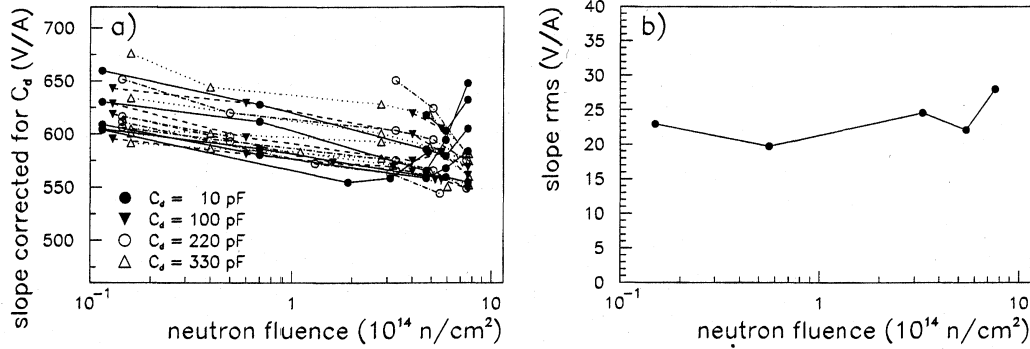


Figure 11: (a) The slope obtained for different detector capacitances in the neutron irradiation of 23 chips at various levels of neutron fluence. (b) The r.m.s of the values as a function of the neutron fluence.

3.3 Equivalent noise current

The equivalent noise current was computed from the measured r.m.s spread of the shaper output voltage in the absence of any input signal by using the measured transfer function. The results are shown in Fig.12 for the neutron irradiation and in Fig.13 for the γ exposure. The equivalent noise current (ENI) is presented for different irradiation levels as a function of the rise time t_p .

Before the irradiation, the noise is the same for the preamplifiers used for the neutron and the γ exposure and it grows with the dose collection. The measured noise is higher for the highest γ dose in comparison with the noise obtained for the maximal neutron fluence. It must be noted that the experimental setup was sensitive to low frequency pick-up noise. Therefore more detailed analysis of the noise behaviour was carried out only for rise time values below 200 ns.

The equivalent noise current could be considered as a sum of series noise and parallel noise and described analytically [4] as

$$ENI = \frac{\alpha}{t_p^{3/2}} \oplus \frac{\beta}{t_p^{1/2}} \quad (1)$$

where α determines the contribution of the series noise and β - the parallel noise. The measured values of equivalent noise current were averaged over the preamplifier channels

with the same detector capacitance and fitted by Eq.1 for different levels of the neutron fluence.

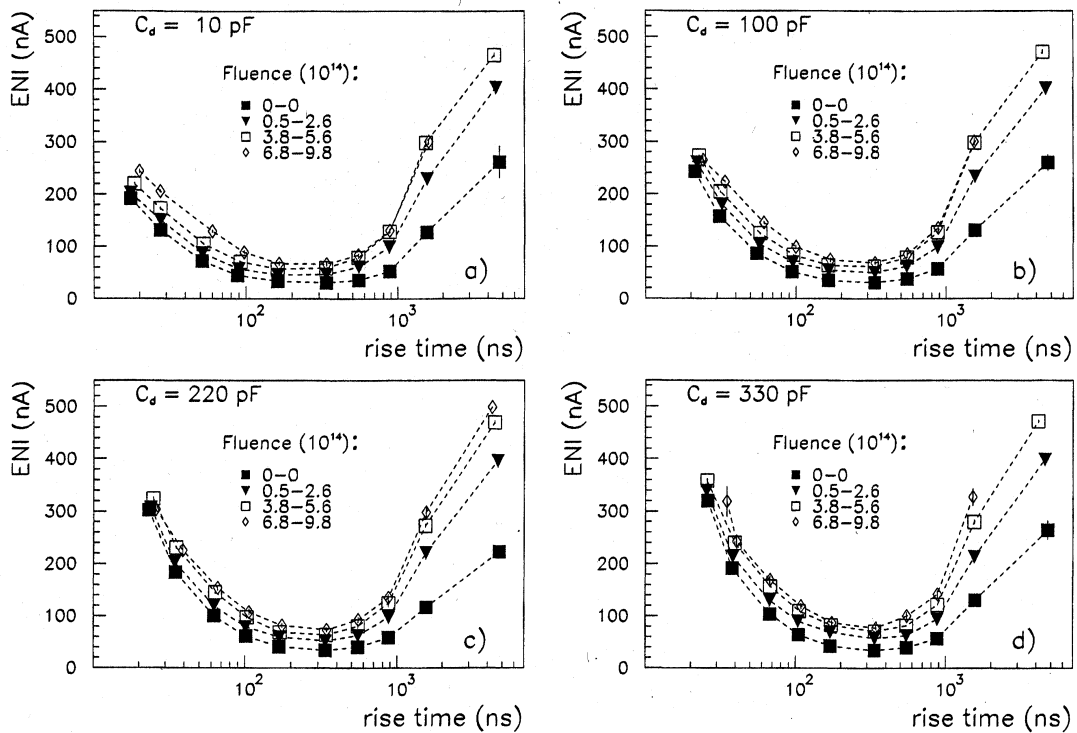


Figure 12: Equivalent noise current as a function of the measured rise time for different levels of the integrated neutron fluence and various values of detector capacitance.

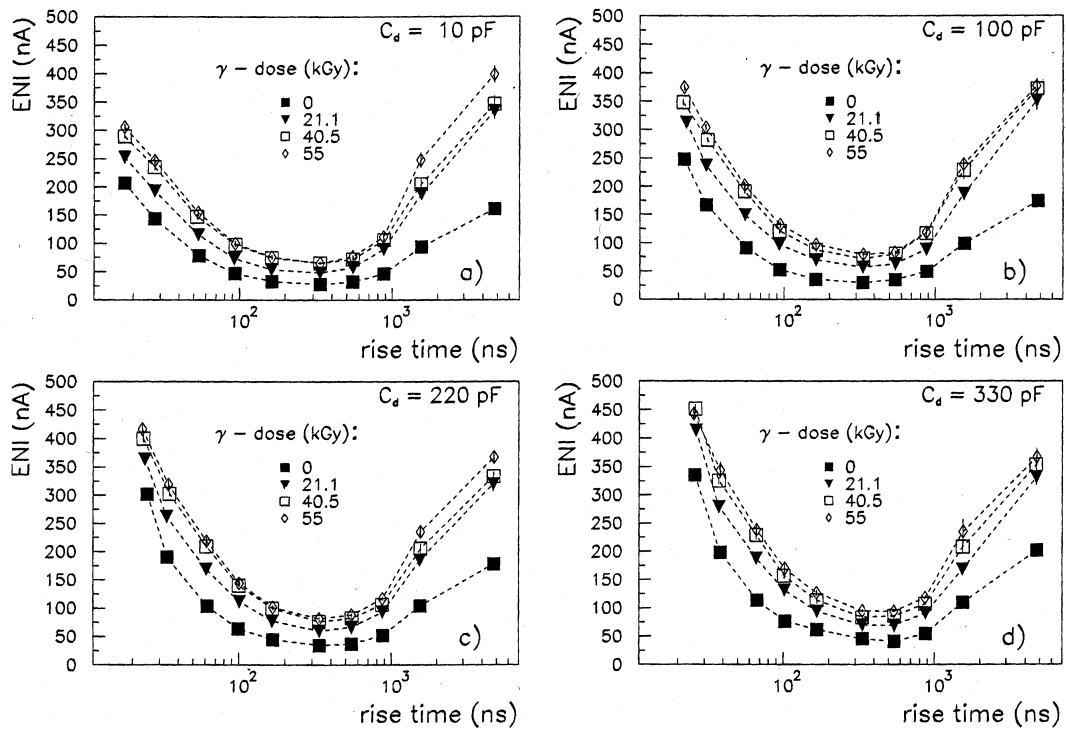


Figure 13: Equivalent noise current as a function of the measured rise time for different levels of the collected γ dose and various values of detector capacitance.

The noise coefficient α derived from the fit of the data obtained before the irradiation run is shown in Fig.14a as a function of the detector capacitance. As expected, it scales with detector capacitance. In Fig.14b the value of α is shown for different C_d values and for various values of the integrated neutron fluence. It is seen that series noise of the preamplifiers is almost stable up to the highest radiation doses.

In Fig.14c the dependence of the fitted parameter β is presented for different C_d as a function of the integrated neutron fluence. At highest irradiation level the parallel noise is two times larger than it was before the irradiation.

The increase of noise with the neutron fluence for a typical rise time value of 40 ns and different detector capacitances is shown in Fig.14d. The equivalent noise current measured during the neutron irradiation is normalised to the value measured before irradiation. The noise is increasing slowly till the fluence of $1 \cdot 10^{14} \text{ n/cm}^2$ independent on the detector capacitance, at $5 \cdot 10^{14} \text{ n/cm}^2$ it exceeds the initial value by 30-50%.

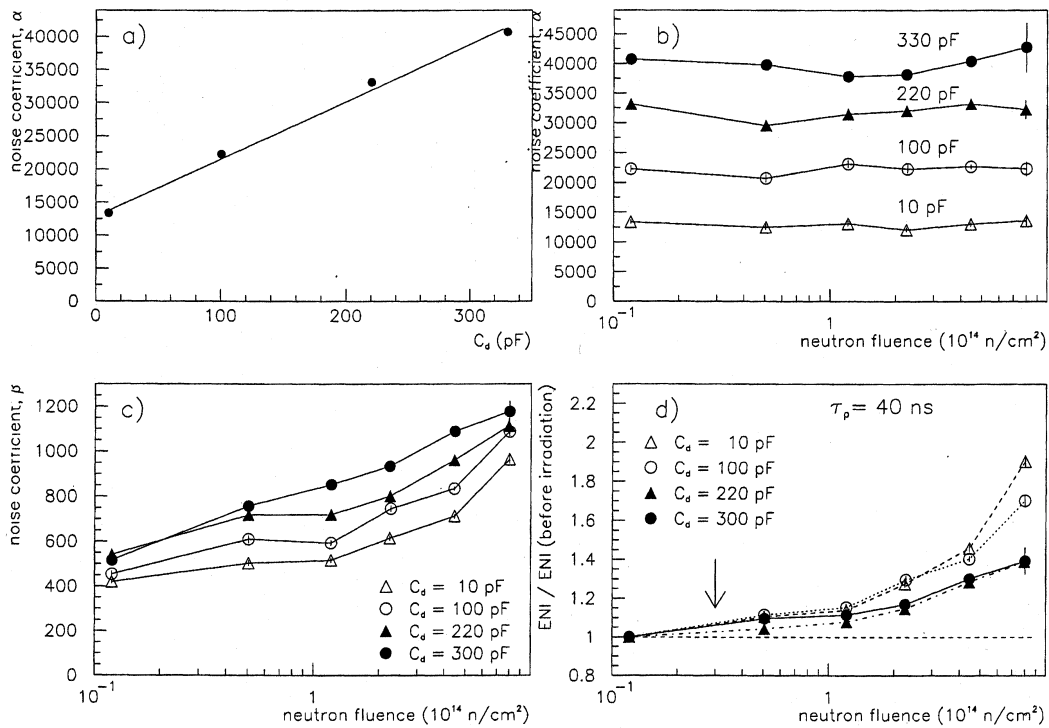


Figure 14: (a) Noise coefficient α derived from the fit of the equivalent noise current by Eq.1 as a function of the detector capacitance C_d before the neutron irradiation. (b) Dependence of the series noise coefficient α on the neutron fluence for different values of C_d . (c) Dependence of the parallel noise coefficient β on the neutron fluence for different values of C_d . (d) The equivalent noise current measured during irradiation normalised to the value measured before irradiation. The data are shown as a function of the neutron fluence for the typical rise time value of 40 ns and different values of the detector capacitance.

The results of the noise analysis are presented in Fig.15 for the γ irradiation. Similar to those, observed for the neutron irradiation, serial noise coefficient α in Eq.1 scales with the detector capacitance and remains almost stable till the highest values of the γ dose. The parallel noise coefficient β is growing significantly with the γ dose. In Fig.15d the equivalent noise current for the rise time of 40 ns is compared with the noise measured before the irradiation. It is seen that under the photon irradiation the noise increases constantly. This is in agreement with the results of the previous experiments with the preamplifier prototypes [2].

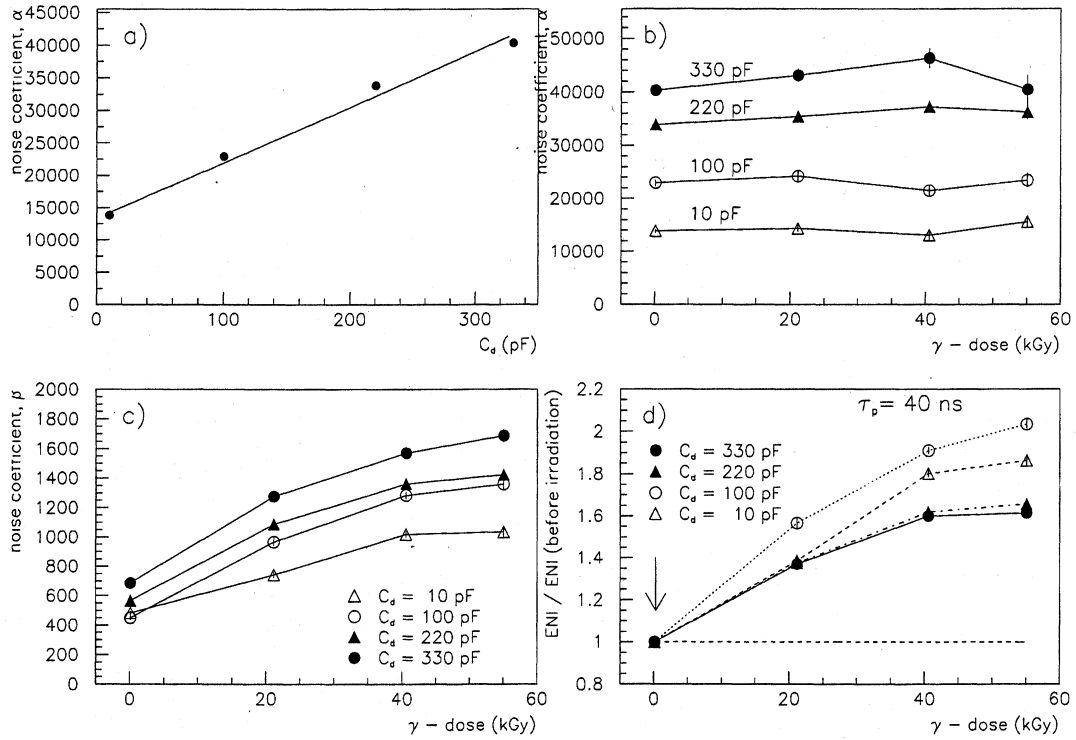


Figure 15: (a) Noise coefficient α derived from the fit of the equivalent noise current by Eq.1 as a function of the detector capacitance C_d before the irradiation by photons. (b) Dependence of the series noise coefficient α on the γ dose for different values of C_d . (c) Dependence of the parallel noise coefficient β on the γ dose for different values of C_d . (d) The equivalent noise current measured during irradiation normalised to the value measured before irradiation. The data are shown as a function of the γ dose for the typical rise time value of 40 ns and different values of the detector capacitance.

4. Conclusions

A series of irradiation tests have been carried out at the IBR-2 reactor in Dubna. The GaAs preamplifiers (final design) which is being used in the hadronic liquid argon end-cap calorimeter of ATLAS were exposed to high neutron fluence and γ dose. In general, the results are in agreement with the previous tests of the preamplifier prototype and measurements performed at different institutes [5]. The preamplifiers show stable performance in terms of transfer function, rise time, noise and linearity up to high neutron fluence of $5 \cdot 10^{14} \text{ n/cm}^2$ independent of the detector capacitance. For the neutron fluence beyond this value a clear deterioration of the transfer function and linearity has been observed.

Under γ irradiation no damage of the performance has been seen up to the maximal accumulated γ dose of 55 kGy.

The equivalent noise current has been found to increase under irradiation by neutrons and photons. The noise increase is more significant under the photon irradiation. It has been found that the noise increase under neutron and photon irradiation is due to an increase of parallel noise, while the series noise remains almost constant till the highest radiation doses.

Nevertheless, the application of the developed electronics for the ATLAS experiment looks uncritical from the radiation hardness point of view. The expected radiation levels at the area of the electronics location (0.3 kGy and $0.3 \cdot 10^{14} \text{ n/cm}^2$ for 10 years of operation at the highest luminosity) are more than an order of magnitude below any critical radiation level.

References

- [1] ATLAS Collaboration
ATLAS Liquid Argon Calorimeter Technical Design Report
CERN/LHCC/96-41 (1996)
- [2] A. Cheplakov et al., ATLAS Internal Note, LARG-96-054 (1996)
- [3] A. Cheplakov et al., HEC-Note, in preparation
- [4] R.L. Chase et al., ATLAS Internal Note, LARG-NO-10 (1995)
- [5] D. V. Camin (RD3 Collaboration), Proc. IV Int. Conf. on Calorimetry in HEP, World Scientific (1994) 618;
M. Citterio, V. Radeka and S. Rescia, Proc. V IEEE Trans. Nucl. Science, Vol.42, No.6 (1995) 2266.